Investigation of 4D dose in volumetric modulated arc therapy-based stereotactic body radiation therapy: does fractional dose or number of arcs matter?

AUTHOR(S):

Shintani, Takashi; Nakamura, Mitsuhiro; Matsuo, Yukinori; Miyabe, Yuki; Mukumoto, Nobutaka; Mitsuyoshi, Takamasa; Iizuka, Yusuke; Mizowaki, Takashi

CITATION:

Shintani, Takashi ...[et al]. Investigation of 4D dose in volumetric modulated arc therapy-based stereotactic body radiation therapy: does fractional dose or number of arcs matter?. Journal of Radiation Research 2020, 61(2): 325-334

ISSUE DATE:

2020-03

URL:

http://hdl.handle.net/2433/250086

Journal of Radiation Research, Vol. 61, No. 2, 2020, pp. 325–334
doi: 10.1093/jrr/rrz103
Advance Access Publication: 6 February 2020

Investigation of 4D dose in volumetric modulated arc therapy-based stereotactic body radiation therapy: does fractional dose or number of arcs matter?

Takashi Shintani[1], Mitsuhiro Nakamura[1,2,*], Yukinori Matsuo[1], Yuki Miyabe[1], Nobutaka Mukumoto[1], Takamasa Mitsuyoshi[1], Yusuke Iizuka[1] and Takashi Mizowaki[1]

[1]Department of Radiation Oncology and Image-applied Therapy, Kyoto University Graduate School of Medicine, 54 Shogoin Kawahara-cho, Sakyo-ku, Kyoto 606-8507, Japan
[2]Division of Medical Physics, Department of Information Technology and Medical Engineering, Human Health Sciences, Graduate School of Medicine, Kyoto University, 53 Kawahara-cho, Shogoin, Sakyo-ku, Kyoto 606-8507, Japan
*Corresponding author. Department of Medical Physics, Department of Information Technology and Medical Engineering, Human Health Sciences, Graduate School of Medicine, Kyoto University, 53 Kawahara-cho, Shogoin, Sakyo-ku, Kyoto 606-8507, Japan. Tel: 075-751-4176; Fax: 075-771-9749; Email: m_nkmr@kuhp.kyoto-u.ac.jp
(Received 26 September 2019; revised 5 December 2019; editorial decision 29 December 2019)

ABSTRACT

The aim of this study was to assess the impact of fractional dose and the number of arcs on interplay effects when volumetric modulated arc therapy (VMAT) is used to treat lung tumors with large respiratory motions. A three (fractional dose of 4, 7.5 or 12.5 Gy) by two (number of arcs, one or two) VMAT plan was created for 10 lung cancer cases. The median 3D tumor motion was 17.9 mm (range: 8.2–27.2 mm). Ten phase-specific subplans were generated by calculating the dose on each respiratory phase computed tomography (CT) scan using temporally assigned VMAT arcs. We performed temporal assignment of VMAT arcs using respiratory information obtained from infrared markers placed on the abdomens of the patients during CT simulations. Each phase-specific dose distribution was deformed onto exhale phase CT scans using contour-based deformable image registration, and a 4D plan was created by dose accumulation. The gross tumor volume dose of each 4D plan (4D GTV dose) was compared with the internal target volume dose of the original plan (3D ITV dose). The near-minimum 4D GTV dose ($D_{99\%}$) was higher than the near-minimum 3D internal target volume (ITV) dose, whereas the near-maximum 4D GTV dose ($D_{1\%}$) was lower than the near-maximum 3D ITV dose. However, the difference was negligible, and thus the 4D GTV dose corresponded well with the 3D ITV dose, regardless of the fractional dose and number of arcs. Therefore, interplay effects were negligible in VMAT-based stereotactic body radiation therapy for lung tumors with large respiratory motions.

Keywords: VMAT-based SBRT; interplay effect; DIR; lung

INTRODUCTION

Stereotactic body radiation therapy (SBRT) can achieve a high local control rate with only rare severe toxicity [1] and is now the standard treatment for inoperable early-stage non-small cell lung cancer [2]. SBRT is a sophisticated irradiation technique in which high-dose radiation is administered accurately in a small number of fractions via a precise patient set-up. The SBRT dose is generally prescribed to the planning target volume (PTV) periphery with a 60–90% isodose to the center of the tumor [3]. In SBRT planning, the internal target volume (ITV) dose is adjusted to be intentionally much higher than the prescription dose because several dose parameters including the prescription dose, PTV mean dose [4] and dose to tumor center [5] are important for achieving sufficient local control.

For the SBRT delivery technique, volumetric modulated arc therapy (VMAT) has been gaining popularity because of its shorter delivery time and better conformity [6]. When utilizing intensity-modulated radiotherapy (IMRT) or VMAT for thoracic tumors, a major concern is interplay effects between multi-leaf collimator (MLC)

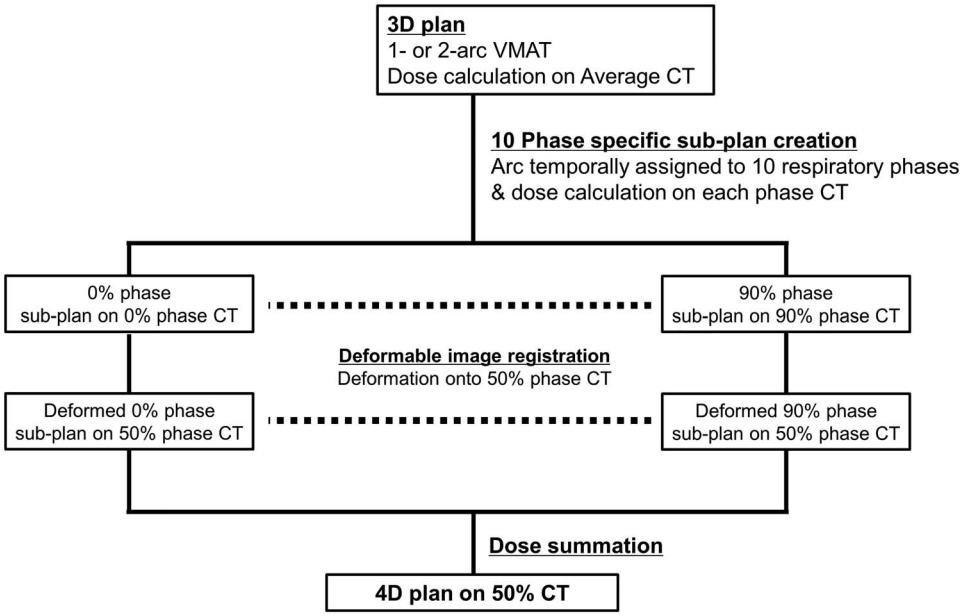

Fig. 1. Schematic illustration showing the creation of the 4D plan. A 3D plan was created and the arc was separated into 10 respiratory phases with the assumption that the arc rotation starts at 0%. Ten phase-specific subplans were created by calculating the dose from the assigned MU on each phase CT scan. Then, each phase-specific subplan was deformed onto the 50% phase CT with the aid of contour-based deformable image registration and dose summation was carried out to create the 4D plan.

motion and a moving tumor that might lead to underdosing the tumor. Respiratory motion-management techniques, such as abdominal compression, respiratory gating, breath-hold and real-time tumor tracking, should be used when treating tumors with large motion [7, 8]. However, if these techniques are not available or are ineffective at reducing the treatment volume, a motion-enveloping method is the only option; interplay effects are thus a matter of concern.

Two methods can be used to explore the impacts of interplay effects on lung IMRT or VMAT: these include experimental phantom studies [9–12] and 4D dose-calculation studies featuring deformable image registration (DIR) [13–15]. These studies have suggested that the interplay effects are negligible under certain conditions. Whether ITV dose metrics truly reflect gross tumor volume (GTV) dose metrics is of clinical interest. We adopted a 4D dose-calculation method rather than an experimental phantom method because, with the former method, it is easier to accumulate doses to a tumor, which can significantly deform during respiration [16]. Although the use of a 3D gel dosimetry phantom would yield accurate dose–volume data for non-rigid targets, such work is rather costly and labor intensive [17].

In this study, we evaluated DIR accuracy and then calculated the magnitude of the interplay effects during VMAT-SBRT of lung tumors exhibiting large motions in various clinically realistic situations. Dose fractionation and the number of VMAT arcs are at the planner's discretion in clinical practice; we focused on these factors in this study. A 3 × 2 (fractional dose of 4, 7.5 or 12.5 Gy × 1 or 2 arcs) VMAT plan was created using the type-C algorithm (fast Monte Carlo dose calculation) which is superior to type-B algorithms (superposition/convolution dose algorithms) for assessing lung dosimetry [18].

MATERIALS AND METHODS

Case selection

We queried our prospectively maintained SBRT database to find lung cancer cases in whom large respiratory motions necessitated motion management, such as real-time tumor-tracking or respiratory gating. Ten peripherally located lung cancer cases with high-quality 4D-computed tomography (CT) images amenable to DIR were included. The study was approved by our institutional review board (approval no. R1446).

CT simulation and target definition

All 4D-CT images were obtained using a 16-slice scanner (Light-Speed RT16; GE Healthcare, Little Chalfont, UK) while respiration was monitored with a real-time position management (RPM) system (Varian Medical Systems, Palo Alto, CA, USA) on the patient's abdomen. The acquisition parameters of the 4D-CT scan were as follows: tube voltage 120 kV, tube current 100 mA, slice thickness 2.5 mm, field-of-view 500 mm, and matrix size 512 × 512. Ten respiratory-phase CT (end-inhale phase corresponds to 0%), average-intensity projection (AIP) and maximum-intensity projection (MIP) images were generated. The GTV was delineated on each respiratory-phase image. The ITV was the summation of the GTVs in all respiratory phases. To avoid underestimation of ITV, we used MIP images as a reference. The PTV was created by adding 5 mm to the ITV.

3D plan creation

Doses were calculated using AIP images. The treatment-planning system was Eclipse (ver. 13.7.29; Varian Medical Systems) and the dose-calculation algorithm was AcurosXB (ver. 13.7.14; Varian Medical

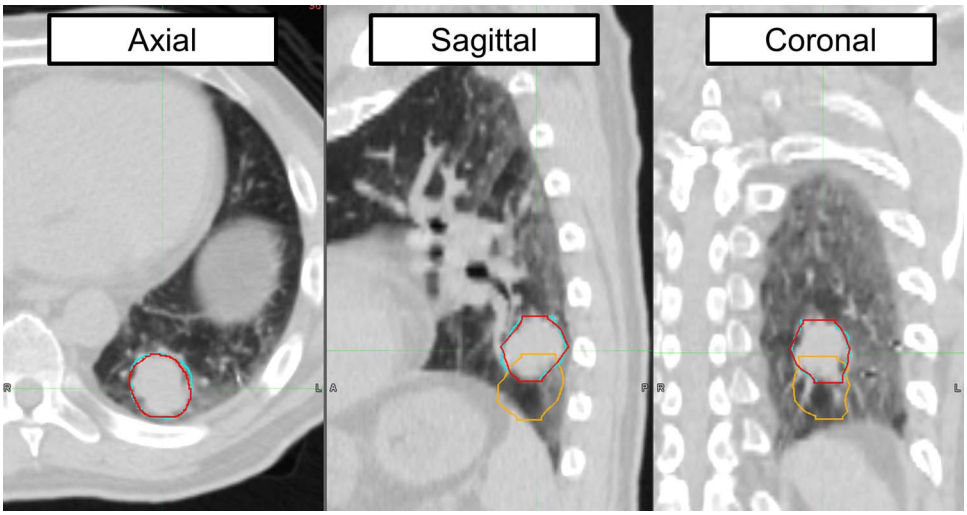

Fig. 2. A representative gross tumor volume (GTV) contour at 50% of the phase and the GTV contour deformed onto 50% of the phase. The original GTV of the 50% phase (exhalation) is shown in red. The original GTV of the 0% phase (inhalation) is shown in orange and the deformation onto the 50% phase CT is shown in cyan. The dice similarity coefficient and mean distance to agreement were 0.94 and 0.44 mm, respectively.

Table 1. Case characteristics (n = 10)

Case no.	1	2	3	4	5	6	7	8	9	10
Tumor location	L	R	L	L	R	R	R	L	R	L
3D tumor motion, mm	8.2	27.2	18.8	8.7	21.7	11.3	21.7	17.4	14.6	18.4
Breathing period, s	3.3	4.3	3.9	3.9	4.5	3.0	6.3	5.9	4.5	3.1
GTV on 10 phase CT										
Mean, mL	7.9	5.2	5.7	5.7	42.8	7.2	6.9	12.7	6.0	4.1
CV	0.14	0.08	0.11	0.05	0.09	0.13	0.05	0.03	0.23	0.16
ITV, mL	15.0	14.6	13.5	10.9	92.3	13.2	16.9	27.3	14.2	11.1
PTV, mL	38.6	41.4	38.7	32.0	169.9	35.6	44.6	61.7	37.6	29.4
One-arc plan										
60 Gy/15fr										
MU	743.9	918.4	816.2	960.4	784.1	941.9	1031.9	1020.4	856.5	961.7
Beam-on time, s	34.8	39.4	36.4	41.2	36.2	40.4	44.2	44.3	37.3	41.2
60 Gy/8fr										
MU	1190.6	1659.2	1835.0	1827.2	1435.6	1729.8	1922.6	1859.7	1633.6	1665.8
Beam-on time, s	51.0	72.7	78.7	78.3	62.0	74.1	82.4	79.7	70.0	71.4
50 Gy/4fr										
MU	2656.0	2694.7	2936.5	3019.1	2505.7	3037.2	3080.3	3395.8	2978.1	2655.5
Beam-on time, s	113.8	115.5	125.8	129.4	107.4	130.2	130.0	145.5	127.6	113.8
Two-arc plan										
60 Gy/15fr										
MU	716.1	785.5	759.7	848.9	777.2	901.1	913.7	1048.7	880.7	861.8
Beam-on time, s	69.7	69.7	69.7	69.7	69.7	69.7	69.7	69.7	69.7	69.7
60 Gy/8fr										
MU	1341.0	1439.0	1616.9	1538.5	1390.8	1775.2	1679.3	1951.0	1648.2	1604.5
Beam-on time, s	69.7	69.7	70.2	69.7	69.7	76.7	72.0	83.6	71.4	70.1
50 Gy/4fr										
MU	2413.6	2446.4	2647.4	2765.4	2432.7	2882.4	2809.6	3074.8	2616.7	2612.5
Beam-on time, s	103.4	104.8	113.5	118.7	104.8	123.6	120.4	132.2	112.1	112.0

L = Left, R = right.

Systems) with a grid size of 2.5 mm. VMAT plans were generated using TrueBeam STx (Varian Medical Systems) with a 6-MV flattening filter-free (FFF) photon beam (maximum dose rate, 1400 monitor units [MU]/min). The central MLC width of the treatment machine was 2.5 mm. The prescription dose was the dose to 95% of the PTV ($D_{95\%}$). The planning objectives were as follows: (i) a maximum dose in the range of 125–140% of the prescription dose and within the ITV; (ii) a $D_{99\%}$ of the PTV >90% of the prescription dose; and (iii) the ITV must receive at least the prescription dose.

Fractional doses of 4 Gy [19], 7.5 Gy [1] and 12.5 Gy [20] were selected as these were utilized in hypofractionated radiotherapy or SBRT in previous studies. We employed one or two arcs. Partial

Table 2. DVH metrics of ITV dose in 3D plan (normalized by prescription dose)

Case no.	1	2	3	4	5	6	7	8	9	10
One-arc plan										
60 Gy/15fr										
$D_{1\%}$, %	134.6	133.7	128.9	132.6	132.9	132.1	138.2	132.4	125.7	134.1
D_{mean}, %	123.2	124.9	120.4	123.9	120.9	121.8	127.8	120.5	119.0	124.5
$D_{99\%}$, %	108.1	112.2	106.1	109.8	104.3	111.3	114.5	106.4	112.8	116.2
60 Gy/8fr										
$D_{1\%}$, %	132.7	134.3	137.2	133.0	132.7	132.6	137.0	133.1	131.1	131.3
D_{mean}, %	121.5	124.9	126.4	123.8	120.2	123.0	125.8	120.8	121.8	123.1
$D_{99\%}$, %	110.0	112.8	114.0	107.8	105.0	110.8	113.5	106.4	114.9	115.1
50 Gy/4fr										
$D_{1\%}$, %	134.8	128.9	132.9	133.7	133.9	131.6	130.9	132.5	127.8	130.9
D_{mean}, %	122.8	120.3	124.4	123.5	120.8	122.4	121.3	121.0	121.1	121.4
$D_{99\%}$, %	108.7	105.6	112.1	107.4	104.3	110.2	108.8	107.2	113.0	113.2
Two-arc plan										
60 Gy/15fr										
$D_{1\%}$, %	133.3	132.4	126.6	136.6	130.7	132.8	131.6	136.8	133.7	129.2
D_{mean}, %	121.7	125.0	120.3	126.2	119.3	123.5	122.3	125.3	125.4	121.0
$D_{99\%}$, %	107.3	115.6	111.8	114.2	106.5	112.5	111.0	112.8	116.1	113.6
60 Gy/8fr										
$D_{1\%}$, %	132.2	136.1	137.7	135.5	130.8	136.3	133.8	135.3	133.7	132.0
D_{mean}, %	120.9	126.9	128.7	126.5	119.4	126.7	123.9	125.0	124.8	123.1
$D_{99\%}$, %	109.9	115.3	116.5	115.4	106.2	114.1	112.1	110.7	115.8	115.6
50 Gy/4fr										
$D_{1\%}$, %	129.7	130.2	130.8	127.6	130.4	134.3	129.7	130.4	128.1	126.9
D_{mean}, %	119.4	119.3	123.4	120.6	118.9	123.2	121.7	121.1	119.9	119.4
$D_{99\%}$, %	107.7	108.7	114.9	113.0	104.5	112.0	112.8	110.6	112.8	112.7

coplanar arcs of 210° were used to avoid beam entry from the contralateral lung. The collimator angle was set at 30 or 330°.

4D planning

Phase-specific subplan creation

Ten phase-specific subplans were made from each plan using the same methods applied for 4D dose calculation by Sasaki *et al.* [21]. In brief, the original digital imaging and communications in medicine–radiation therapy (DICOM-RT) plan file was first obtained. In this DICOM-RT file, each arc contained 114 control points (CPs) representing the beam parameters, including gantry angles, MLC positions, dose rates and MU per gantry rotation. Using this information, we calculated the time from beam delivery onset to each CP. According to the respiratory information on RPM, we temporally assigned VMAT arcs to 10 respiratory phases. We made the assumption that the beam rotation started at 0% (Fig. 1). We made this assumption because the beam starting phase does not have a significant influence on the 4D dose in VMAT plans, either in the setting of SBRT or in conventionally fractionated radiotherapy [13–15, 21]. This procedure was carried out using C++ language. Then, the treatment plans with split arcs were imported back into the treatment planning system (Eclipse) in DICOM format, and dose calculation was conducted based on the assigned-phase CT scan.

Dose deformation of the phase-specific subplan using contour-based deformable image registration

Phase-specific subplans were deformed to 50% phase CT scans using MIM software version 6.8.3 (MIM Software Inc., Cleveland, OH, USA) with contour-based DIR. The GTV of each phase of CT was delineated manually by a single board-certified radiation oncologist and was used for DIR because our main interest was to estimate the dose to the GTV. The 50% phase CT scan was selected as the reference image because the exhale phase is the most stable and free from artifacts.

As DIR quality is critically important in terms of dose deformation, the accuracy of DIR was confirmed both via visual inspection and quantitatively, and the uncertainty levels were scored as suggested in the American Association of Physicists in Medicine (AAPM) Report 132 [22]. On visual inspection, a score of 0–4 was assigned for registration accuracy, where 0 represented perfect registration and 4 unusable registration. The dice similarity coefficient (DSC) and mean distance to agreement (MDA) were the quantitative methods employed. The DSC is defined as twice the overlapping volume of the GTV at 50% of the phase and the GTV of the remaining phase after deformation of the 50% phase CT data divided by the total volume of both contours. The MDA is the average distance between the GTV at 50% of the phase and the deformed GTV of the remaining phase. We considered that a DSC >0.8 and MDA <2 mm reflected contour uncertainty [21].

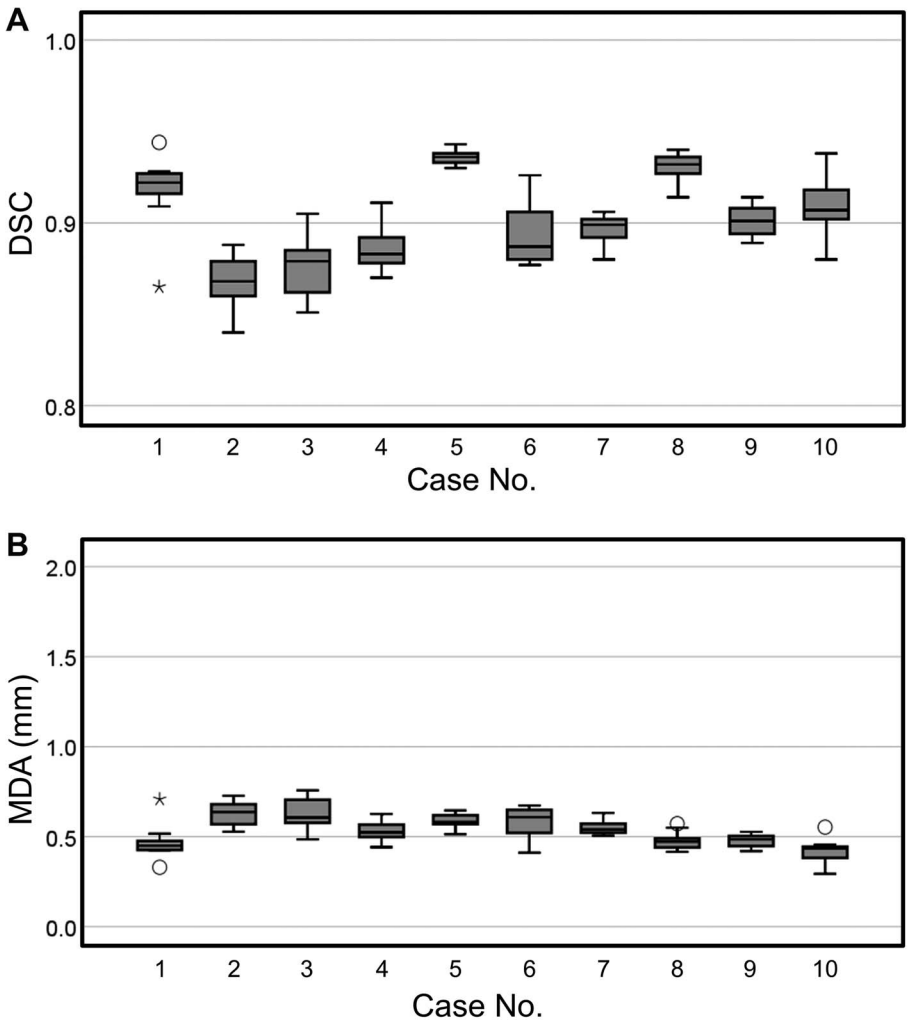

Fig. 3. Box and whisker plot of the dice similarity coefficient (DSC) (a) and mean distance to agreement (MDA) (b) between the GTV at 50% of the CT phase and the other GTV phase (after deformation onto the 50% phase CT data). The box length is the interquartile range with bisecting lines showing the median values. The small circles and asterisks represent outliers.

4D plan creation via dose summation of deformed phase-specific subplans and comparison of the 4D GTV and 3D ITV doses

Each 4D plan was created by calculating the summed dose of the 10 deformed phase-specific subplans (Figs 1 and 2). The dose to the GTV in the 4D plan (the 4D GTV dose) was compared with the dose to the ITV in the 3D plan (the 3D ITV dose). The dose–volume histogram (DVH) metrics evaluated were $D_{99\%}$, the mean dose (D_{mean}) and $D_{1\%}$. $D_{99\%}$ and $D_{1\%}$ served as surrogates of the near-minimum and near-maximum doses since point-minimum and point-maximum doses are more susceptible to uncertainty in terms of the DIR, target delineation and dose calculation. For simplicity, we defined R_x as follows:

$$R_x = D_x \text{ of 4D GTV dose}/D_x \text{ of 3D ITV dose.} \quad (1)$$

Rx and Dx should be italic (R and D, not subscript x) in the equation R_x in three different fractional doses was compared using repeated measures analysis of variance. R_x was compared between one and two arcs using the same fractional dose set with paired *t*-tests. Comparisons were two-sided and $P < 0.05$ was deemed significant.

Then, we assessed the impact of the number of respirations using Spearman's rank correlation. The number of respirations was calculated by dividing the beam-on time by the average breathing period of each patient. First, we assessed the association between the number of respirations and the coefficient of variation (CV) of the MU value assigned to each subplan, which was calculated as follows:

$$\mathrm{CV} = \sigma/M, \quad (2)$$

where σ and M are the standard deviation and mean value of the MU value assigned to the10 phase-specific subplans, respectively.

Then, we analysed the association of the number of respirations with R_x.

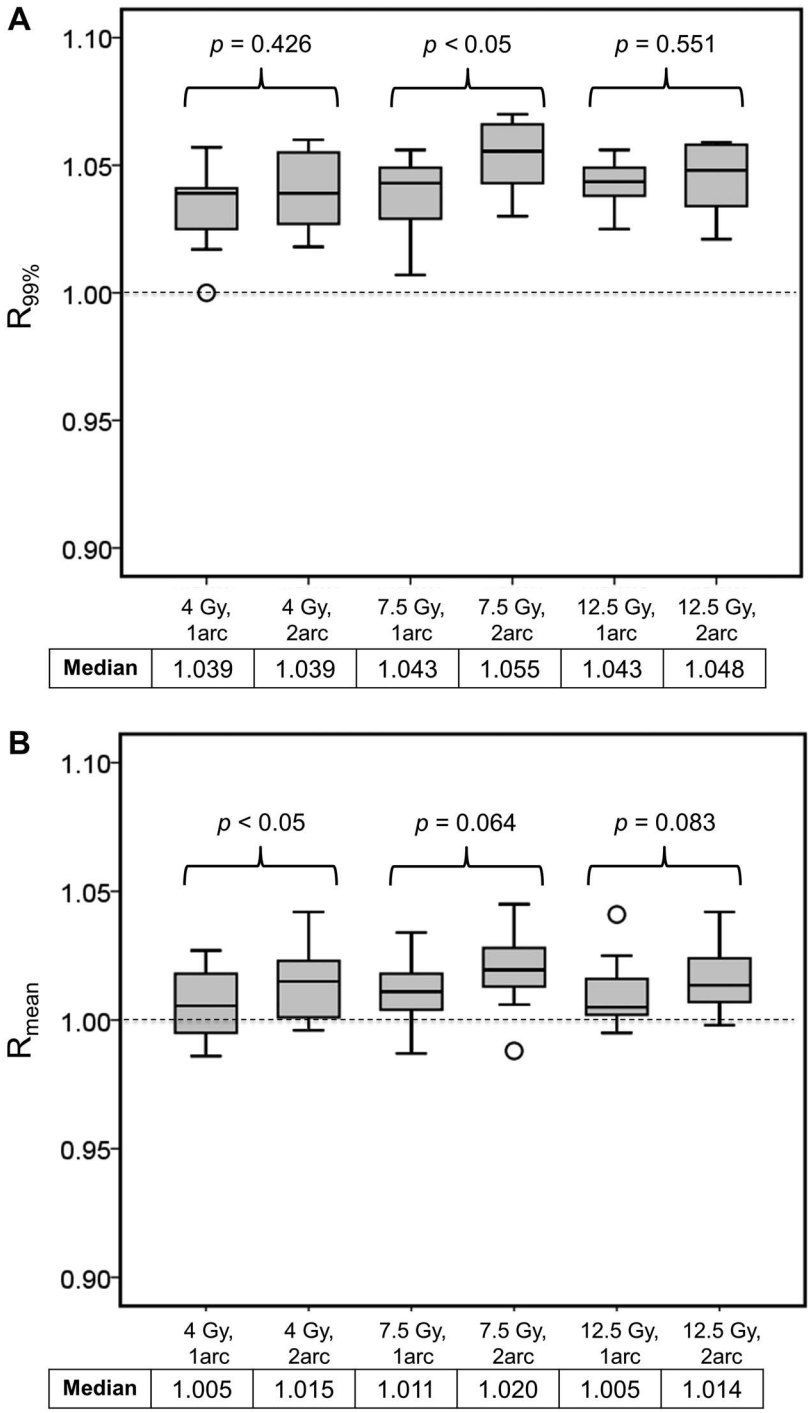

Fig. 4. Box and whisker plots of $R_{99\%}$ (a), R_{mean} (b) and $R_{1\%}$ (c) are shown. The box length is the interquartile range with bisecting lines showing the median values. The small circles represent outliers. The *P*-values were obtained using the paired-*t* test. $R_x = D_x$ of 4D GTV dose/D_x of 3D ITV dose.

RESULTS

Case characteristics

Table 1 shows the case characteristics. The median 3D tumor motion was 17.9 mm (range: 8.2–27.2 mm) and the median PTV volume was 38.7 cc (range: 29.4–169.9 cc). In the two-arc plan, the median beam-on time, which was estimated from the beam CPs and gantry rotation speed, was 69.7 s (range: 69.7–69.7 s), 70.2 s (range: 69.7–83.6 s) and 112.8 s (range: 103.4–132.2 s) for fractional doses of 4 7.5 and 12.5 Gy,

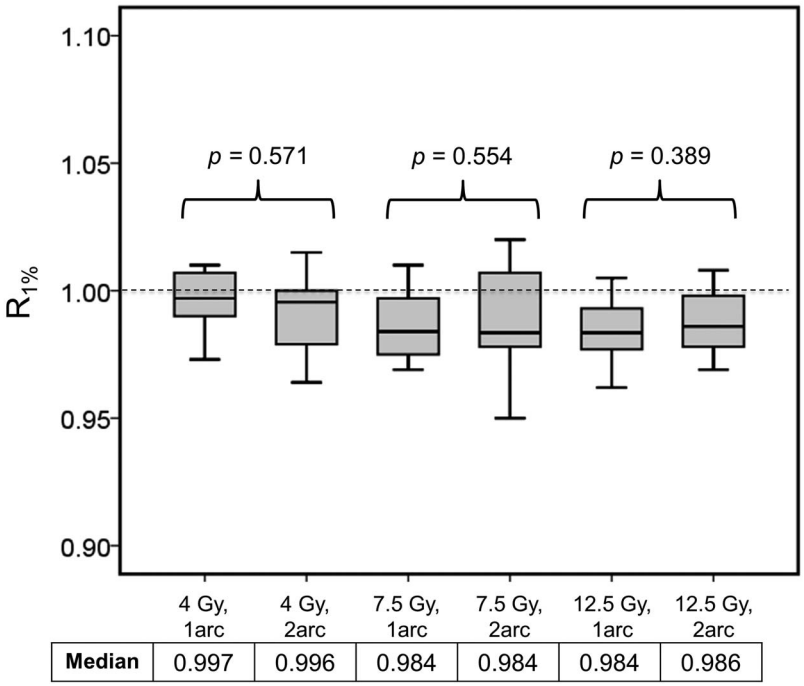

Fig. 4. continued.

respectively. In the one-arc plan, the respective median beam-on-time was 39.9 s (range: 34.8–44.3 s), 73.4 s (range: 51.0–82.4 s) and 126.7 s (range: 107.4–145.5 s). In Table 2, the DVH metrics of ITV are shown for each plan.

Assessment of DIR accuracy

A representative comparison of GTV contours is shown in Fig. 2. The DSC and MDA for each case are shown in Fig. 3. Both the DSC and MDA met our criteria (DSC > 0.8 and MDA < 2 mm). The DIR accuracy was 1 in all DIRs, according to the AAPM Report 132 [22]. Thus, local alignment around the GTV was good.

4D GTV dose vs 3D ITV dose

Impact of fractional dose

The $R_{99\%}$, R_{mean} and $R_{1\%}$ data are shown in Fig. 4. $R_{99\%}$, R_{mean} and $R_{1\%}$ were not statistically different among the three different fractional doses in either the one-arc plan (P = 0.81, 0.11 and 0.66, respectively) or the two-arc plan (P = 0.57, 0.97 and 0.38, respectively).

Impact of arc number (one arc vs two arcs)

At a fractional dose of 7.5 Gy, $R_{99\%}$ was statistically higher for the two-arc than the one-arc plan ($P < 0.05$), but the difference was small (median value: 1.055 vs 1.043). With a fractional dose of 4 Gy, the R_{mean} was statistically higher in the two-arc plan than in the one-arc plan ($P < 0.05$), but this difference was also minimal (median, 1.015 vs 1.005). Other DVH metrics were not statistically different between the one- and two-arc plans, as shown in Fig. 4.

Association of the number of respirations with the CV of the MU

The median number of breaths during the beam-on time was 18.6 (range: 7.0–43.4). The circles in Fig. 5(a) refer to 60 plans (three different fractional doses delivered via one or two arcs to 10 patients) and are coded depending on the CV of the MU value assigned to each phase and the number of breaths. A larger number of respirations was associated with a lower CV of the MU ($r = -0.541$, $P < 0.001$). There was a significant correlation between R_{mean} and the number of respirations ($r = 0.318$, $P = 0.013$) [Fig. 5(a)]. $R_{99\%}$ and $R_{1\%}$ showed no significant correlation with the number of respirations, as illustrated in Fig. 5b and d.

DISCUSSION

We showed that the DVH metrics of the 4D GTV dose corresponded well with those of the 3D ITV dose regardless of the fractional dose or number of arcs, even in cases with large respiratory motion.

The cases included in this study had much larger tumor motion (median 3D motion. 17.9 mm) than reported in previous studies [13, 14]. In thoracic regions showing large motion, DIR accuracy can be compromised by unusual case characteristics or DIR maneuvers [23–25]. To overcome this problem, we used contour-based DIR, and thereby obtained DIR images for which both the DSC and MDA values were well within the levels of contour uncertainty, as shown in Fig. 2.

As for fractional dose, whether interplay effects are negligible in IMRT or VMAT plans with small fractional doses is a matter of controversy [9, 13]. Plan complexity could be instructive in this respect, as shown by Court *et al.* [26]. They evaluated interplay effects with a conventionally fractionated radiotherapy plan (2 Gy/fraction

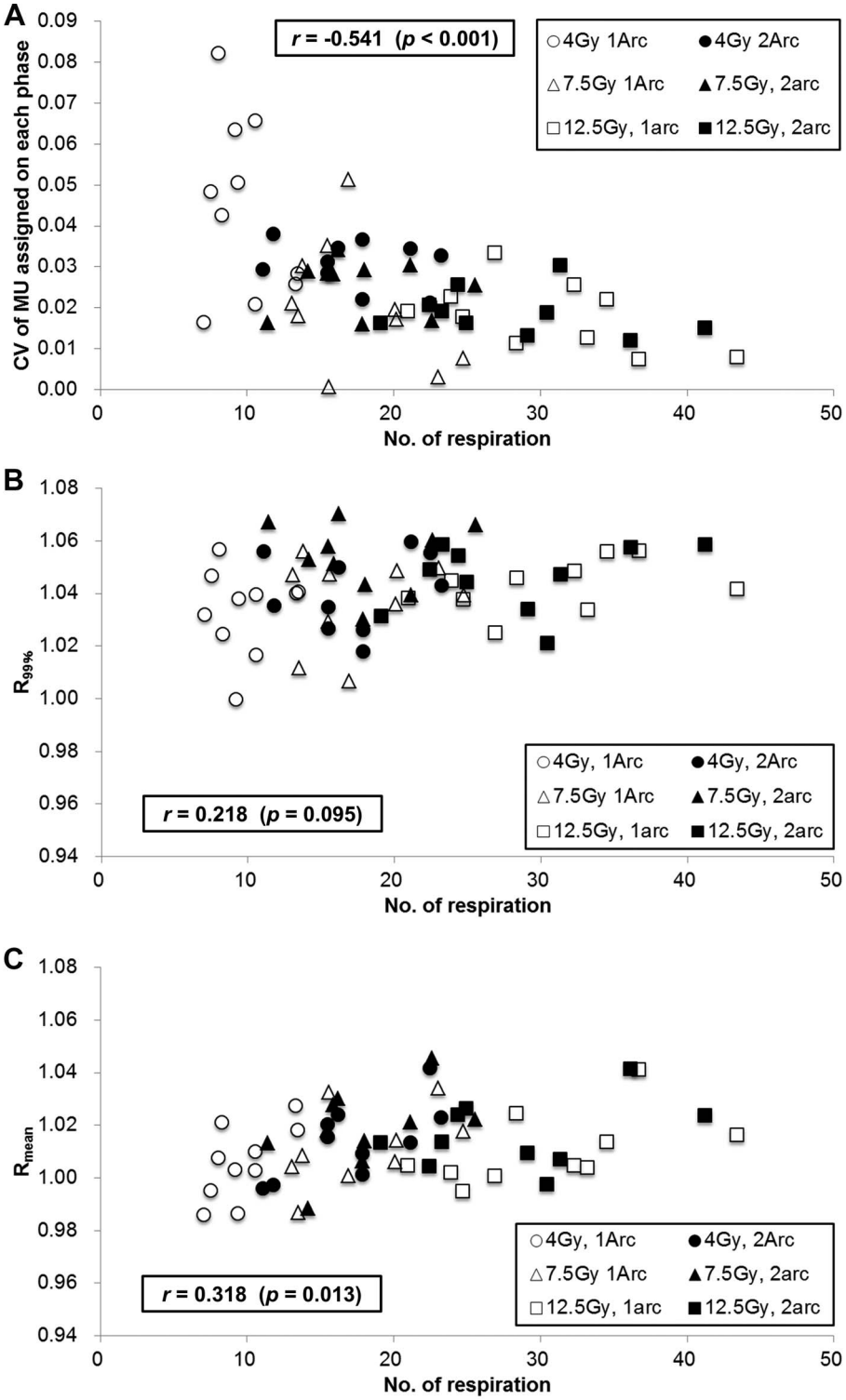

Fig. 5. Correlations between the number of breaths and the coefficient of variation (CV) of the monitor units (MU) assigned to each phase (a). A larger number of respirations is associated with a lower CV of the MU ($r = -0.541$, $P < 0.001$). The correlation between the number of breaths and R_x is shown in (b–d). We found no significant correlation between the number of breaths and the $R_{99\%}$ (a) or $R_{1\%}$ (c) ratio. A correlation was evident between the number of breaths and the R_{mean} ratio (b), but the strength of the correlation was weak ($r = 0.318$, $P = 0.013$). $R_x = D_x$ of 4D GTV dose/D_x of 3D ITV dose.

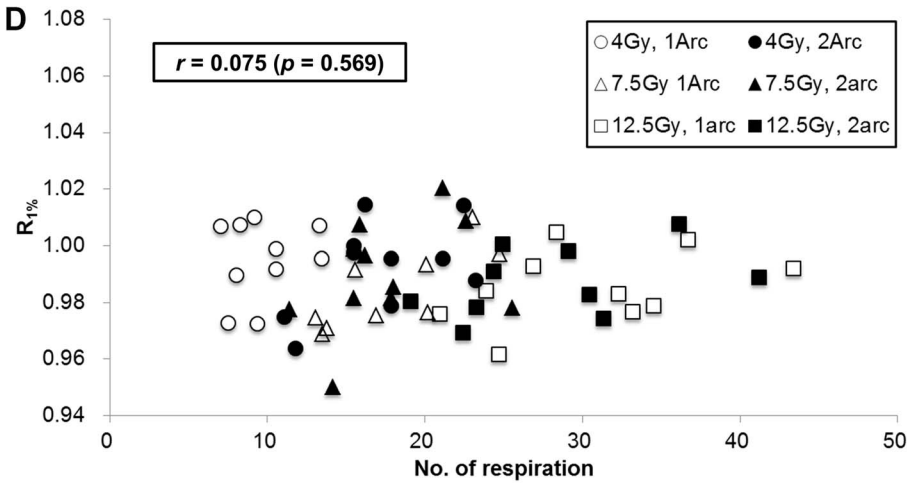

Fig. 5. continued.

(fr)) delivered by various treatment techniques (step-and-shoot IMRT, dynamic IMRT and RapidArc) and found that interplay is significant only in clinically unrealistic complex plans. Thus, the reason that we did not observe large interplay effects even with a small fractional dose (4 Gy/fraction) could be that the cases included in our study had peripherally located tumors that were not in close proximity to the bronchial tree or large vessels and the complexity of the 3D treatment plans was generally low.

Regarding the number of arcs, both the current and previous 4D dose-estimation studies suggest that the volumetric dose to 4D GTV is almost same as that to 3D ITV. In this study, although $R_{99\%}$ for a fractional dose of 7.5 Gy, and R_{mean} for a fractional dose of 4 Gy, showed a statistical difference between the 1- and 2-arc plans, the magnitude of the difference was quite small. However, the small volumetric difference between the 3D and 4D plans does not rule out a point dose difference. For example, in their phantom study, Ong *et al*. showed that the maximum dose deviation in the PTV between 1- and 2-arc plans was 5–10%, but the deviation became smaller for the 2-arc plan [11]. Considering that phantom and 4D dose calculation studies complement each other, from a conservative point of view, it might be better to adopt double-arc delivery because the delivery time with a double-arc plan is still short and within the clinically acceptable range.

A long motion period has been reported to trigger a large interplay effect [27]. We hypothesized that a small number of respirations during beam-on time might lead to uneven assignment of MU to each plan and thus create a large difference between the 4D GTV and 3D ITV doses. As expected, variations of MU among plans were larger when there was a small number of breaths during irradiation. However, the number of respirations did not greatly influence the final dose. We observed a statistical correlation between the D_{mean} ratio and number of breaths, but the strength of the correlation was only modest ($r = 0.318$).

Our study had several limitations. First, although we confirmed the accuracy of DIR using the best available method, voxel-by-voxel matching within the GTV is not guaranteed. Second, while our study revealed that the tumor dose is almost the same as the planned dose to ITV, this does not mean that a respiratory motion-management technique is unnecessary. This is because the dose to organs at risk is known to be a predictor of toxicity such as radiation pneumonitis [28] and chest wall toxicity [29]. Third, in cases with large motion, the breathing motion during treatment can be different from that during CT simulation [30], so caution is needed when interpreting our results in the context of clinical practice. Fourth, although beyond the scope of this study, other treatment parameters might also affect 4D dosimetry. Such parameters could also interact, so it may be difficult to assess their individual impacts. In this study, we created clinically realistic, rather than complex, plans, and found that the 4D GTV and 3D ITV doses were similar in such plans, regardless of the fractional dose and number of arcs. It should be noted that the number of samples was small because the creation of 4D plans is labor-intensive. Nevertheless, we can still conclude that there is no meaningful difference, if any, between the 3D ITV and 4D GTV doses.

In summary, we showed that the accuracy of DIR was sufficiently high to allow us to evaluate 4D doses calculated using a type-C algorithm; the 4D GTV doses were comparable with the 3D ITV doses for 10 lung cancer cases exhibiting large respiratory motions, regardless of the fractional dose and number of arcs. Interplay effects were negligible in VMAT-based SBRT for peripherally located lung tumors with large respiratory motion.

CONFLICT OF INTEREST

None declared.

FUNDING

This work was supported in part by Japan Society for the Promotion of Science KAKENHI (Grant Nos. 18H02766 and 18 K15630).

ACKNOWLEDGMENTS

We thank Euro Meditech and MIM Software Inc. for allowing us to use MIM Maestro.

REFERENCES

1. Senthi S, Lagerwaard FJ, Haasbeek CJA et al. Patterns of disease recurrence after stereotactic ablative radiotherapy for early stage non-small-cell lung cancer: A retrospective analysis. *The Lancet Oncology* 2012;13:802–9.
2. Videtic GMM, Donington J, Giuliani M et al. Stereotactic body radiation therapy for early-stage non-small cell lung cancer: Executive summary of an ASTRO evidence-based guideline. *Pract Radiat Oncol* 2017;7:295–301.
3. Chang JY, Bezjak A, Mornex F et al. Stereotactic ablative radiotherapy for centrally located early stage non-small-cell lung cancer: What we have learned. *J Thorac Oncol* 2015;10:577–85.
4. Zhao L, Zhou S, Balter P et al. Planning target volume D_{95} and mean dose should be considered for optimal local control for stereotactic ablative radiation therapy. *Int J Radiat Oncol Biol Phys* 2016;95:1226–35.
5. Mehta N, King CR, Agazaryan N et al. Stereotactic body radiation therapy and 3-dimensional conformal radiotherapy for stage I non-small cell lung cancer: A pooled analysis of biological equivalent dose and local control. *Pract Radiat Oncol* 2012;2: 288–95.
6. Zhang GG, Ku L, Dilling TJ et al. Volumetric modulated arc planning for lung stereotactic body radiotherapy using conventional and unflattened photon beams: A dosimetric comparison with 3D technique. *Radiat Oncol* 2011;152:1–6.
7. Brandner ED, Chetty IJ, Giaddui TG et al. Motion management strategies and technical issues associated with stereotactic body radiotherapy of thoracic and upper abdominal tumors: A review from NRG oncology. *Med Phys* 2017;44:2595–612.
8. Keall PJ, Mageras GS, Balter JM et al. The management of respiratory motion in radiation oncology report of AAPM task group 76. *Med Phys* 2006;33:3874–900.
9. Jiang SB, Pope C, Al Jarrah KM et al. An experimental investigation on intra-fractional organ motion effects in lung IMRT treatments. *Phys Med Biol* 2003;48:1773–84.
10. Tyler MK. Quantification of interplay and gradient effects for lung stereotactic ablative radiotherapy (SABR) treatments. *J Appl Clin Med Phys* 2016;17:158–66.
11. Ong CL, Dahele M, Slotman BJ et al. Dosimetric impact of the interplay effect during stereotactic lung radiation therapy delivery using flattening filter-free beams and volumetric modulated arc therapy. *Int J Radiat Oncol Biol Phys* 2013;86:743–8.
12. Stambaugh C, Nelms BE, Dilling T et al. Experimentally studied dynamic dose interplay does not meaningfully affect target dose in VMAT SBRT lung treatments. *Med Phys* 2013;40:091710.
13. Rao M, Wu J, Cao D et al. Dosimetric impact of breathing motion in lung stereotactic body radiotherapy treatment using image-modulated radiotherapy and volumetric modulated arc therapy. *Int J Radiat Oncol Biol Phys* 2012;83:e251–6.
14. Ehrbar S, Johl A, Tartas A et al. ITV, mid-ventilation, gating or couch tracking - a comparison of respiratory motion-management techniques based on 4D dose calculations. *Radiother Oncol* 2017;124:80–8.
15. Li X, Yang Y, Li T et al. Dosimetric effect of respiratory motion on volumetric-modulated arc therapy-based lung SBRT treatment delivered by TrueBeam machine with flattening filter-free beam. *J Appl Clin Med Phys* 2013;14:195–204.
16. Senthi S, Dahele M, Slotman BJ et al. Investigating strategies to reduce toxicity in stereotactic ablative radiotherapy for central lung tumors. *Acta Oncol* 2014;53:330–5.
17. Ceberg S, Ceberg C, Falk M et al. Evaluation of breathing interplay effects during VMAT by using 3D gel measurements. *Journal of Physics: Conference Series.* 2013;444:012098.
18. Zhou C, Bennion N, Ma R et al. A comprehensive dosimetric study on switching from a type-B to a type-C dose algorithm for modern lung SBRT. *Radiat Oncol* 2017;12:80.
19. Cheung P, Faria S, Ahmed S et al. Phase II study of accelerated hypofractionated three-dimensional conformal radiotherapy for stage T1-3 N0 M0 non-small cell lung cancer: NCIC CTG BR. *25. J Natl Cancer Inst* 2014;106:1–8.
20. Chang JY, Li QQ, Xu QY et al. Stereotactic ablative radiation therapy for centrally located early stage or isolated parenchymal recurrences of non-small cell lung cancer: How to fly in a no fly zone. *Int J Radiat Oncol Biol Phys* 2014;88:1120–8.
21. Sasaki M, Nakamura M, Mukumoto N et al. Variation in accumulated dose of volumetric-modulated arc therapy for pancreatic cancer due to different beam starting phases. *J Appl Cli Med Phys* 2019;20:118–26.
22. Brock KK, Mutic S, McNutt TR et al. Use of image registration and fusion algorithms and techniques in radiotherapy: Report of the aapm radiation therapy committee task group no. *132. Med Phys* 2017;44:e43–76.
23. Sarudis S, Karlsson A, Bibac D et al. Evaluation of deformable image registration accuracy for CT images of the thorax region. *Phys Med.* 2019;57:191–9.
24. Guy CL, Weiss E, Che S et al. Evaluation of image registration accuracy for tumor and organs at risk in the thorax for compliance with TG 132 recommendations. *Adv Radiat Oncol.* 2019;4:177–85.
25. Mogadas N, Sothmann T, Knopp T et al. Influence of deformable image registration on 4D dose simulation for extracranial SBRT: A multi-registration framework study. *Radiother Oncol.* 2018;127:225–32.
26. Court LE, Seco J, Lu XQ et al. Use of a realistic breathing lung phantom to evaluate dose delivery errors. *Med Phys* 2010; 37:5850–7.
27. Court LE, Wagar M, Ionascu D et al. Management of the interplay effect when using dynamic MLC sequences to treat moving targets. *Med Phys.* 2008;35:1926–31.
28. Matsuo Y, Shibuya K, Nakamura M et al. Dose-volume metrics associated with radiation pneumonitis after stereotactic body radiation therapy for lung cancer. *Int J Radiat Oncol Biol Phys* 2012;83:e545–9.
29. Stephans KL, Djemil T, Tendulkar RD et al. Prediction of chest wall toxicity from lung stereotactic body radiotherapy (SBRT). *Int J Radiat Oncol Biol Phys* 2012;82:974–80.
30. Dhont J, Vandemeulebroucke J, Burghelea M et al. The long- and short-term variability of breathing induced tumor motion in lung and liver over the course of a radiotherapy treatment. *Radiother Oncol* 2018;126:339–46.